

# Spectroscopic time-resolved diffuse reflectance and transmittance measurements of the female breast at different interfiber distances

## Antonio Pifferi

Politecnico di Milano  
ULTRAS-INFM, INF-CNR  
Dipartimento di Fisica  
P. L. da Vinci 32  
I-20133 Milano  
Italy  
E-mail: antonio.pifferi@fisi.polimi.it

## Johannes Swartling

Politecnico di Milano  
Dipartimento di Fisica  
P. L. da Vinci 32  
I-20133 Milano  
Italy  
and  
Lund University Medical Laser Centre  
Department of Physics  
Lund Institute of Technology  
P.O. Box 118  
SE-221 00 Lund  
Sweden

## Ekaterine Chikoidze Alessandro Torricelli Paola Taroni

Andrea Bassi  
Politecnico de Milano  
ULTRAS-INFM, INF-CNR  
Dipartimento di Fisica  
P. L. da Vinci 32  
I-20133 Milano  
Italy

## Stefan Andersson-Engels

Lund University Medical Laser Centre  
Department of Physics  
Lund Institute of Technology  
P.O. Box 118  
SE-221 00 Lund  
Sweden

## Rinaldo Cubeddu

Politecnico de Milano  
ULTRAS-INFM, INF-CNR  
Dipartimento di Fisica  
P. L. da Vinci 32  
I-20133 Milano  
Italy

## 1 Introduction

Measurements of the absorption coefficient  $\mu_a$  and the reduced scattering coefficient  $\mu'_s$  of turbid media have become an important part of the developing field of tissue optics. Optical measurements can be performed *in vivo* noninvasively on patients, and new techniques are emerging as feasible meth-

**Abstract.** The first, to our knowledge, *in-vivo* broadband spectroscopic characterization of breast tissue using different interfiber distances as well as transmittance measurements is presented. Absorption and scattering properties are measured on six healthy subjects, using time-resolved diffuse spectroscopy and an inverse model based on the diffusion equation. Wavelength-tunable picosecond-pulse lasers and time-correlated single-photon counting detection are employed, enabling fully spectroscopic measurements in the range 610 to 1040 nm. Characterization of the absorption and reduced scattering coefficients of breast tissue is made with the aim of investigating individual variations, as well as variations due to different measurement geometries. Diffuse reflectance measurements at different interfiber distances (2, 3, and 4 cm) are performed, as well as measurements in transmittance mode, meaning that different sampling volumes are involved. The results show a large variation in the absorption and scattering properties depending on the subject, correlating mainly with the water versus lipid content of the breast. Intra-subject variations, due to different interfiber distances or transmittance modes, correlate with the known structures of the breast, but these variations are small compared to the subject-to-subject variation. The intrasubject variations are larger for the scattering data than the absorption data; this is consistent with different spatial localization of the measurements of these parameters, which is explained by the photon migration theory. © 2004 Society of Photo-Optical Instrumentation Engineers.

[DOI: 10.1117/1.1802171]

Keywords: time-resolved spectroscopy; scattering; absorption; optical mammography; breast.

Paper 94001 received Dec. 2, 2003; revised manuscript received Feb. 12, 2004; accepted for publication Feb. 13, 2004.

ods for diagnostics of some pathological conditions. An additional advantage of optical methods is that they pose no known health risks, in contrast to, for example, x-rays. Special attention has been directed to the possibility of detecting cancer tumors in breasts.<sup>1–8</sup> When applied using a spectroscopic approach, optical methods in the red and near-infrared (NIR) region provide the means to yield functional information of the tissue, specifically the abundance of oxygenated

Address all correspondence to Antonio Pifferi, Politecnico di Milano, Dipartimento di Fisica, Piazza Leonardo da Vinci 32, I-20133 Milan, Italy. Tel: 39-02-23-99-61-09; Fax: 39-02-23-99-61-26; E-mail: antonio.pifferi@fisi.polimi.it

(HbO<sub>2</sub>) and deoxygenated hemoglobin (HHb), water, and fat.<sup>3,7,9–12</sup> This information could be used to develop contrast functions to distinguish malignant tissue. The scattering properties can also potentially provide information on malignancy, because the scattering coefficient will be affected by structural changes of the tissue. The task of optical mammography is thus to evaluate the optical properties over the breast volume. An important part of this development is to be able to accurately measure the optical properties locally. Spectroscopic *in-vivo* measurements of this kind have been performed to determine the parameter range of  $\mu_a$  and  $\mu'_s$  for healthy tissue, which is strongly influenced by factors such as age and hormonal cycle,<sup>11,13–17</sup> and body mass index (BMI).<sup>8,17,18</sup> The measurement techniques employed are usually either based on frequency-modulated light sources<sup>8,11,19,20</sup> or time-resolved diffuse spectroscopy.<sup>3,7,13,21,22</sup> Absorption and scattering coefficients can be determined from the measurements by means of an inverse model based on a theoretical model for light propagation in tissue, such as diffusion theory.<sup>22–24</sup> The structures in the breast are a heterogeneous mix of glandular and adipose tissues. In general, the breast structure of young women is characterized by dense, glandular, and thus water-rich tissue. The postmenopausal breast, in contrast, presents a reduction in the glandular volume, and the relative amount of adipose tissue increases. However, these general characteristics are obscured by a large subject-to-subject variation, and for an individual one cannot identify the type of breast based on the age. When performing noninvasive measurements *in vivo*, the skin layer presents an additional type of tissue with its own scattering and absorption properties.

Previous phantom studies have concluded that the accuracy of the time-resolved technique and homogeneous tissue model is better than 10% for homogeneous samples.<sup>24,25</sup> However, there is a growing concern that heterogeneities in tissue may result in higher uncertainty. In this work, measurements of the optical properties of *in-vivo* breast tissue are presented for six subjects, comprising different breast types ranging from water-rich to lipid-rich. The *in-vivo* measurements were performed in reflectance geometry using different interfiber distances,  $\rho$ , and in transmittance geometry. Thus different sampling depths were probed. The measurement system used in this work gives spectra over the range 610 to 1040 nm every 5 nm. This is in contrast to most previous diffuse NIR investigations of breast tissue, which have relied on a small number of discrete wavelengths. Although in principle only four wavelengths are necessary to recover the four major absorbers in breast tissue—water, lipids, oxygen-saturated (HbO<sub>2</sub>) and nonoxygen-saturated hemoglobin (HHb)—access to whole spectra makes the spectral fitting procedure more robust with respect to noise and measurements errors.

It is our intention to show the effects of different measurement geometries, as well as the features of the spectra, and discuss them in a qualitative way. The number of subjects is not enough to provide statistical information, but some important insights of the variation of optical properties of breast tissue can nevertheless be acquired. We also feel that presenting full absorption and scattering spectra yields valuable information to researchers in the field of optical mammography, which may be difficult to obtain when only a few discrete wavelengths are used.

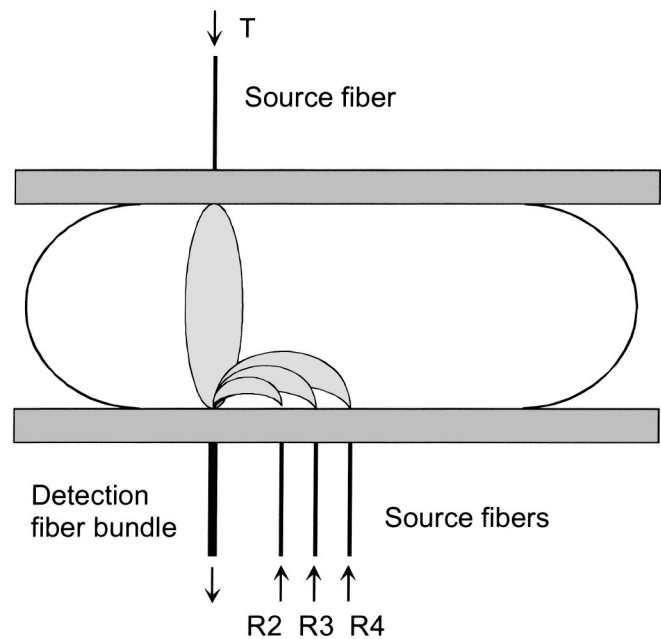


**Fig. 1** Picture showing the measurement geometry. R2, R3, and R4 denotes the reflectance modes for  $\rho=2, 3,$  and  $4$  cm, respectively. T denotes the transmittance measurement. The sampling volumes of the propagating light are schematically depicted for each case.

## 2 Material and Methods

### 2.1 Measurement Protocol

Six healthy volunteers [23, 29, 31, 34, 40, and 50 years old, with body mass indices (BMI) of 22.2, 18.7, 21.3, 19.0, 18.4, and 21.2 kg/m<sup>2</sup>, respectively] were enrolled for the measurements after informed consent. No particular preselection of the volunteers was done, although in some cases the approximate optical signals were known from previous investigations. The volunteers were sitting in an upright position. The breast was placed between two plates, corresponding to the cranio-caudal projection in mammography, and mild compression was applied. The pressure was just enough to keep the breast in a stable position, and much lower than used for radiomammography. The compression did not cause discomfort during the  $\sim 30$ -min measurement session. Measurements were performed in reflectance mode in the area of the upper outer quadrant using different interfiber distances:  $\rho=2, 3,$  and  $4$  cm, denoted R2, R3, and R4 according to Fig. 1. A transmission measurement was also performed at the same time, denoted T in Fig. 1. The thickness of the breast during compression was noted to be used later in the evaluation model. For one volunteer, age 40, two measurement series were performed, where in the first, no compression was applied to the breast during the measurements, and in the second, mild compression was applied during all measurements. This was to present an idea of the effect of different measurement procedures on the measured optical properties.

### 2.2 Time-Resolved Spectroscopy System

The system setup has been described in previous publications.<sup>13,14</sup> Briefly, a synchronously pumped mode-locked dye (DCM) laser was used as the excitation source

from 610 to 695 nm, while an actively mode-locked Ti:sapphire laser provided light in the wavelength range of 700 to 1040 nm. A 1-mm plastic-glass fiber (AFS1000, Fiberguide, New Jersey) delivered light into the tissue, while diffusely reflected photons were collected by a 5-mm-diam fiber bundle. The power at the distal end of the illumination fiber was always limited to less than 10 mW. For detection, we used a double-microchannel-plate photomultiplier tube (R1564U with S1 photocathode, Hamamatsu Photonics K.K., Japan), and a PC card for time-correlated single-photon counting (SPC-130, Becker and Hickl GmbH, Germany). A small fraction of the incident beam was coupled directly to the photomultiplier tube to account for on-line recording of the instrument response function (IRF). The full width at half maximum (FWHM) of the IRF was <120 ps in the red and <180 ps in the NIR regions, respectively. Time-resolved data were collected every 5 nm from 610 to 1040 nm. To allow measurements to be carried out *in vivo*, the system was fully automated. A PC controlled the laser tuning and power, and optimized the IRF by automatically adjusting the Lyot filters and, for the Ti:sapphire laser, the cavity length.

Measurements were performed in reflectance mode (three measurements) and in transmittance mode (one measurement) according to the schematic picture in Fig. 1. All four measurements were performed sequentially before tuning to the next wavelength. This was accomplished by using an optical fiber switch (F109, Piezo Jena, Germany) on the light-source side, also controlled automatically by the PC. In this way, all four measurement geometries were covered in a quasi-parallel manner. A single measurement at one position and wavelength took 2 s. The overall measurement time for a full spectrum, four geometries, was 30 min. To handle the large dynamic range these measurements present, a gradient ND filter was mounted on a stepper motor in the detection line to adjust the intensity on the detector. The total number of photons counted per second was used as input in a feedback loop, and we aimed at having a signal of 300,000 counts/s.

The combination of a thick breast and/or high absorption resulted in too low of a signal for a small number of the measurements. In case only a small part of the spectrum was lost for this reason, the spectrum was still used to make the fit for tissue composition.

### 2.3 Evaluation of Time-Resolved Data

We extracted the values of  $\mu'_s$  and  $\mu_a$  at each wavelength by fitting the experimental data to an analytical solution of the diffusion approximation of the transport equation for a homogeneous semi-infinite medium or an infinite slab.<sup>23</sup> We used the extrapolated boundary condition,<sup>26</sup> and assumed that the diffusion coefficient  $D$  [i.e.,  $D = 1/(3\mu'_s)$ ] was independent of the absorption properties of the medium.<sup>27</sup> The theoretical time-dispersion curve was convolved with the IRF and normalized to the area of the experimental curve. The fitting range included all points with a number of counts higher than 80% of the peak value on the rising edge of the curve and 1% on the tail.<sup>24</sup> The best fit was reached with a Levenberg-Marquardt algorithm<sup>28</sup> by varying both  $\mu'_s$  and  $\mu_a$  to minimize the error norm  $\chi^2$ .

### 2.4 Tissue Composition and Structure

To evaluate the percentage composition of tissues, the absorption spectra were fitted with a linear combination of the spectra of the main tissue constituents, i.e., lipid, water, HbO<sub>2</sub>, and HHb:

$$\mu_a = \sum_i c_i \varepsilon_i(\lambda), \quad (1)$$

where  $\lambda$  is the wavelength,  $c_i$  is the concentration (free fit parameter), and  $\varepsilon_i(\lambda)$  is the specific absorption of the  $i$ 'th constituent. To this purpose, the spectra of water,<sup>29</sup> HHb, and HbO<sub>2</sub><sup>9</sup> were obtained from the literature, while the authors have measured the absorption spectra of lipid (lard) previously.<sup>13</sup> The knowledge of the absorption properties of the two forms of hemoglobin allowed us also to evaluate the total hemoglobin content  $tHb = [HHb] + [HbO_2]$  and the hemoglobin oxygen saturation  $StO_2 = [HbO_2]/\{[HHb] + [HbO_2]\}$ . These properties were evaluated for all subjects at different interfiber distances and for the transmittance geometry.

The dependence of the scattering coefficient on the wavelength can be approximated by a power law derived, empirically, from the Mie theory.<sup>30,31</sup> A function of the type

$$\mu'_s = a\lambda^{-b} \quad (2)$$

was fitted to the scattering spectra. The exponent  $b$  (i.e., the slope of the spectrum in a logarithmic scale) is related to the mean effective size of scattering centers, while the amplitude  $a$  is affected mainly by the density of scattering centers. Thus, a higher value of  $b$  corresponds to smaller effective scattering centers, characterized by a steeper slope of the spectrum. The fit was made in the wavelength range 705 to 930 nm. The reason is that the power law approximation is less valid below 700 nm,<sup>31</sup> and above 930 nm the evaluated scattering coefficients were sometimes influenced by a slight cross talk with the absorption coefficient, due to the peak in the water absorption spectrum.

## 3 Results and Discussion

### 3.1 Absorption Properties

Absorption spectra for all subjects in the transmittance geometry are shown in Fig. 2. The solid lines indicate the fitted spectra based on reference spectra for water, lipids, HHb, and HbO<sub>2</sub>. The evaluated concentrations of these constituents are shown in the table set within the diagram. The subjects are identified by the numerals 1 to 6, and have been ordered from water-rich to lipid-rich according to the results in the table. It is evident that a large individual variation is prevalent in the absorption spectra from these six subjects, especially so in the wavelength region above 930 nm. The large spectral differences above 930 nm are due to a strong variation in the water and lipid content of the breasts of the six subjects. One can identify a continuous distribution of breast types from water-rich (62% water, 16% lipids) to lipid-rich (12% water, 68% lipids). Breasts that are typically water-rich may be expected to have different tissue-structural composition than the typically lipid-rich, which is an important point to keep in mind in further discussion. At 970 nm, the absorption is 3.2 times

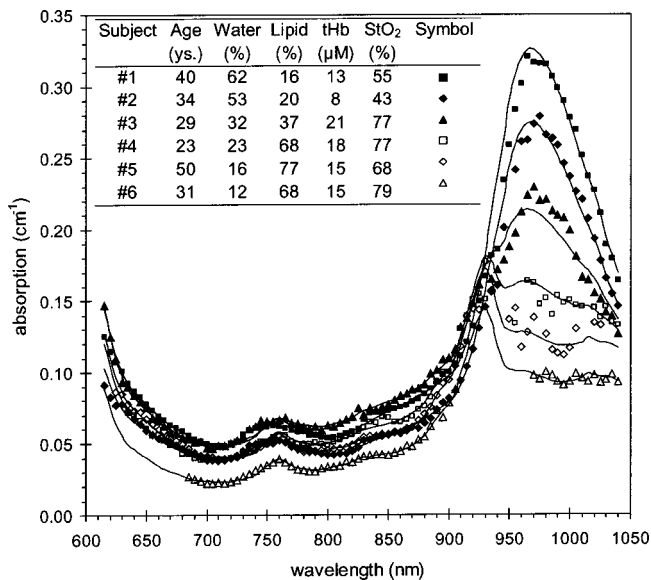


**Fig. 2** Absorption spectra for all subjects using the transmittance geometry. Markers indicate measurements, while solid lines show the fitted spectra. The results from the fitting are shown in the table. Missing data points were due to the combination of a thick breast and high absorption or scattering, resulting in low signal.

stronger for subject 1 than subject 6, due to the higher water absorption. In the region below 930 nm, the influence of the water and lipid absorption is less evident. However, by comparing with the absorption spectra for the pure tissue constituents, it is clear that the water and lipid absorption contribute to the total absorption by a significant amount even for shorter wavelengths. For example, for subject 1, at 750 nm the contribution of absorption by water is 38% of the total, and 4% by lipid. For subject 6 the values are 9% for water and 23% for lipid. At 850 nm, the corresponding values are 43% for water and 2% for lipid (subject 1), and 12% for water 11% for lipid (subject 6). The contribution of water and lipid together falls below 10% at 660 nm, and for shorter wavelengths the tHb absorption quickly becomes dominant. Since the water and lipid contents are the major source of intersubject variation, while HHb and HbO<sub>2</sub> vary less, we conclude that the spectral influence of water and lipid is important in the entire range 700 to 1050 nm. The errors that arise in the evaluation of HHb and HbO<sub>2</sub>, if the absorption of water and lipid is ignored, have been discussed in detail by Cerussi et al.<sup>16</sup>

For this small number of subjects there is no evident correlation between age and optical properties. On the contrary, very large differences are found within the group of subjects around 30 years old. Cerussi et al. have shown a statistical correlation of age versus water and lipid content based on larger statistical material,<sup>15</sup> but on an individual basis the variation is too large for age to be a useful identifier of breast type. Moreover, analysis of radiological breast patterns confirms a general evolution toward more adipose tissue with age, but also in that case the intersubject variations are commonly more significant. For BMI, one can observe that the three subjects with BMI values below 20 kg/m<sup>2</sup> belong to the water-rich category (1, 2, and 3), while the other three with BMI > 20 kg/m<sup>2</sup> belong to the lipid-rich. This supports the

hypothesis of a correlation between BMI and breast tissue types. However, for larger statistical material, only a weak correlation between BMI and measured water or lipid content has been demonstrated previously.<sup>17</sup>

Another interesting spectral feature is the existence of a quasi-isosbestic point at around 930 nm, where the variation is minimal. This can be explained by the crossing of the water and lipid spectra, which makes the absorption largely invariant to changes in the relative amounts of water and lipids around this wavelength, provided that the sum of the volume fractions of water and lipid does not vary substantially. The variation that still exists around this wavelength can be ascribed to two things. First, variations in the hemoglobin absorption, but this variation is smaller than for water/lipid, in part due to smaller differences in HHb and HbO<sub>2</sub> concentrations, and in part due to that the absorption of these chromophores is small compared to that of water and lipid. Second, the isosbestic property depends on the sum of water and lipid content being constant. This may not be true, for example, if there is a significant percentage volume of structural proteins that is not constant. As is discussed later, the sum of water and lipid does not generally add up to 100%. Since the amount of structural proteins in the tissue is likely to vary, this can account for variations in the absorption. For the transmission measurements, the sum of water and lipids varied approximately between 70 to 90%. This means that the isosbestic feature of the absorption spectra at 930 nm is only approximate. Nevertheless, the quasi-isosbestic point may be practically useful because the absorption is invariant to the relative amounts of water and lipid, and thus breast type. This gives approximate upper and lower limits of the absorption one can expect from measurements at 930 nm, and can be used as a quick check that the measurement gives reasonable values. The transmission measurements were in the interval  $0.15 < \mu_a < 0.18 \text{ cm}^{-1}$  at 930 nm. Another useful feature of this point could be to serve as *a priori* information for use in fitting data using various photon migration models. For example, in case cw measurements are carried out, it could be useful to fix the absorption coefficient at 930 nm to get an estimate of the scattering coefficient.

Absorption spectra for all subjects and measurement geometries are shown in Figs. 3(a) through 3(f). The distribution covering water-rich to lipid-rich breast types is very clear when regarding the relative heights of the lipid and water absorption peaks (approximately 930 and 970 nm, respectively). In terms of differences between the various measurement geometries, the results are somewhat inconclusive regarding trends of the individual chromophores. There is a general trend that the water and lipid content increases when going from  $\rho = 2 \text{ cm}$  to  $\rho = 3 \text{ cm}$  in most subjects. It is clear that the sum of water and lipid increases as the interfiber increases from 2 to 4 cm: from between 62 to 76% at  $\rho = 2 \text{ cm}$  to between 73 to 100% for  $\rho = 4 \text{ cm}$ . This likely indicates the presence of a higher percentage volume of proteins such as collagen in the dermis layer, which is sampled to a higher degree for  $\rho = 2 \text{ cm}$ . In general, the unaccounted matter can be due to structural proteins in the tissue. One must be cautious not to draw too quantitative conclusions about the unaccounted matter, since errors in the evaluated values can occur because of the heterogeneous structures that are probed

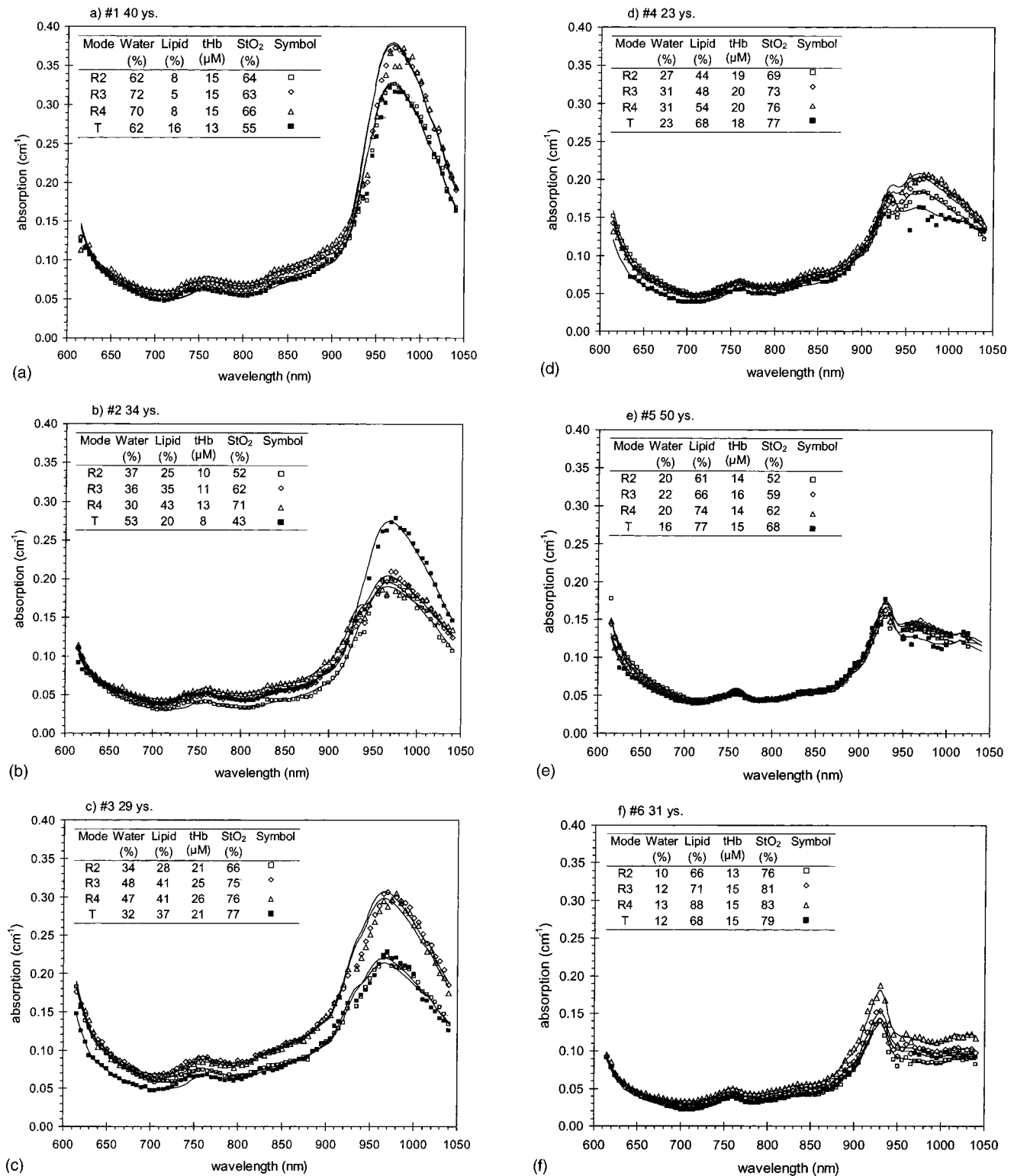


**Fig. 3** All absorption spectra: (a) subject 1, 40 years old; (b) subject 2, 34 years old; (c) subject 3, 29 years old; (d) subject 4, 23 years old; (e) subject 5, 50 years old; and (f) subject 6, 31 years old.

by the light. Unaccounted matter of the order of 10 to 40% of the volume has been reported previously based on photon migration measurements.<sup>14,15,32</sup> The transmittance measurements generally show a lower water contribution than the  $\rho = 4$ -cm measurements, which may seem surprising given that

one would expect the water-rich glandular tissue to be sampled to a greater extent in transmittance. Still, the sampling volume of the propagating light, the influence of the tissues inside this volume, and how the homogenous model weighs the different contributions are complicated issues and

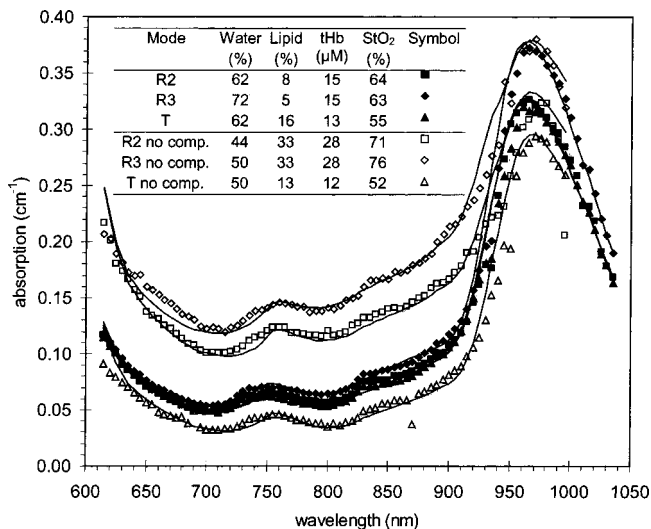


**Fig. 4** Absorption spectra for subject 1, showing the difference between compressed and noncompressed breast during the measurements. The measurement for  $\rho=4$  cm could not be performed in the noncompressed case (not shown in the compressed case either), due to too low of a signal.

not necessarily intuitive. The sampling volumes will also be discussed in Sec. 3.2 on scattering properties.

The most notable observation from the absorption spectra for the different measurement geometries is that, despite some variation, the general characteristics are relatively similar for different geometries. Thus, for the sampling volumes used in this investigation, the intrasubject variation is much smaller than the intersubject variation. This means that measurements performed using a given geometry can indeed be used to confidently characterize the general breast tissue properties in studies on patients or volunteers, although one cannot directly compare the absolute values from measurements taken using one geometry with those taken using another.

In Fig. 4, the difference between no compression and mild compression is shown. Data for  $\rho=4$  cm in the noncompressed case could not be recorded because the signal was too low. The major difference for noncompressed compared to compressed is that the absorption increases due to increased hemoglobin absorption for the reflectance measurements, resulting in roughly a two-fold increase in absorption in the region 610 to 850 nm. This is likely due to influence of the chest muscle. In the case of compression, influence from the chest muscle was largely eliminated, but when applied with no compression the probe was directed toward the chest, perpendicular to the skin surface, and was also considerably closer to the muscular tissue. *In-vivo* measurements on the arm, mainly probing the muscle, normally result in  $\mu_a \approx 0.2 \text{ cm}^{-1}$  at 700 nm.<sup>33</sup> The absorption properties of the chest muscle can be expected to be similar to the muscles in the arm. The absorption values for the uncompressed case in Fig. 4, at around  $0.12 \text{ cm}^{-1}$  at 700 nm, thus fits with the interpretation that the measurement is influenced by the muscle. It is unlikely that the lower hemoglobin absorption in the compressed case was a result of decreased blood perfusion, since the compression was mild. The influence of pressure on the optical properties of breast tissue has been inves-

tigated by Jiang et al., and their results showed that the changes in absorption were relatively small, on the order of 10 to 20% even for large pressure.<sup>34</sup> Furthermore, the absorption due to hemoglobin actually increased, possibly due to vasodilatation. This again indicates that the high absorption for noncompressed breast in our study is due to the presence of the muscle. In the transmittance geometry, the values from the two measurements are comparable. This is reasonable, since to make this measurement possible the breast had to be compressed to some extent even for the noncompressed case. The results in Fig. 4 indicate that control of the application of the probe is important and may influence the measured properties.

### 3.2 Scattering Properties

Spectra of the reduced scattering coefficient are shown in Fig. 5 for all subjects in the transmittance geometry. The values of the fitted parameters  $a$  and  $b$  are presented in the table set within the figure. We can clearly see two groups that correlate with the breast types: the three most water-rich breasts have slope factors  $b$  of 2.0, 2.0, and 1.4. In contrast, the three more lipid-rich breasts are all at  $b$  values of 0.7. For comparison, it is of interest to note that we measured  $b=2.9$  for pure, *ex-vivo* (bovine) cartilage, where the high value is due to the small scattering centers of collagen. The high values of  $b$  thus correlate well with the observation that water-rich breasts are to a large extent made up of collagen structures that support the mammary gland. Fatty tissues, on the other hand, have larger scattering centers and thus lower values of  $b$  ( $b=0.7$  for subjects 4, 5, and 6). Figure 6 shows correlation plots of water and lipid content versus the slope factor  $b$ . This demonstrates that there is a clear positive correlation between water content and  $b$ , while there is a clear negative correlation for lipid content versus  $b$ . Similar results have been shown previously by other investigators.<sup>15</sup> Again, this points to the conclusion that water-abundant breasts are associated with a larger influence of the collagen-rich glandular tissue. Similar plots were obtained for the reflectance modes (data not shown). Both scattering amplitude  $a$  and the slope factor  $b$  have been shown to correlate well with the radiographic density of breast tissue,<sup>17</sup> which is consistent with the interpretation that high radiographic density is due to water-rich, fibrous breasts. The amplitude factor  $a$  is related to the density of scatterers, but also to their size, which makes it difficult to make a simple physical interpretation of the significance of  $a$ . Correlations for both  $a$  and  $b$  with various physiological parameters in breast tissue have been discussed in Ref. 17.

Scattering spectra for all subjects and measurement geometries are presented in Figs. 7(a) through 7(f). The distribution covering water-rich to lipid-rich breasts is evident, here because of the steeper slopes of the spectra for subjects 1, 2, and 3, not only for the transmittance geometry, as already shown in Fig. 4, but also for the reflectance measurements at all interfiber distances. This variation of water- to lipid-rich breasts was also observed in the absorption properties (Fig. 2). However, in contrast to the case for the absorption data, it is possible to clearly distinguish the transmittance measurements from the reflectance measurements. A generally higher scattering coefficient is an indication that different structures in the breast are probed in the transmittance geometry.

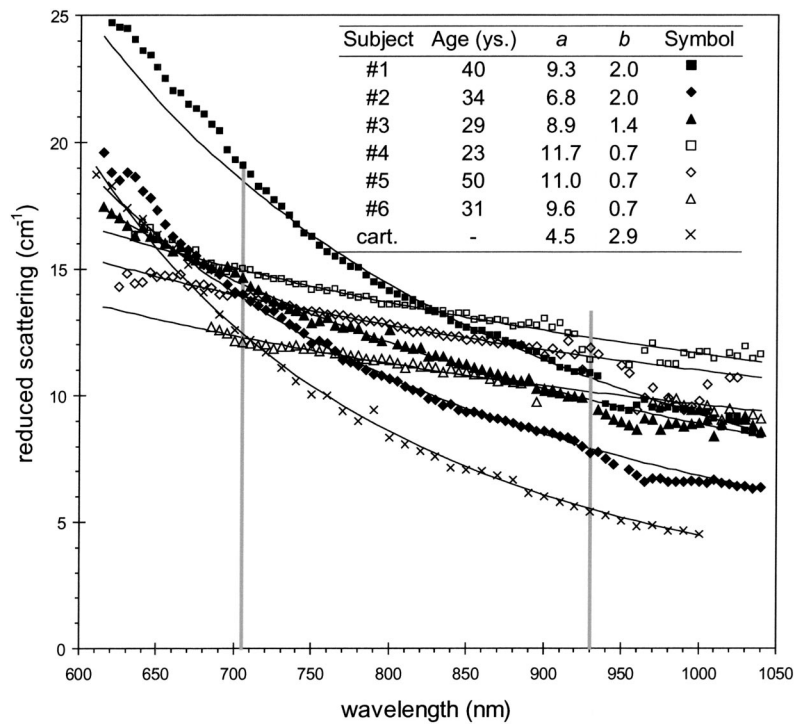


Fig. 5 Spectra of the reduced scattering coefficient for all six subjects, for the transmittance geometry. The scattering spectrum of cartilage is also shown for comparison.

In reflectance, there is a clear trend of decreasing values of  $b$  when going from short interfiber distances to large. One can speculate that the high values of  $b$  found for  $\rho=2$  cm is a result of largely sampling the collagen-rich dermis layer. There is no conclusive trend for the behavior of  $b$  at different  $\rho$  for the different breast types, water-rich or lipid-rich, except that  $b$  is generally higher for the water-rich. In transmittance mode, the value of  $b$  is higher than for reflectance,  $\rho=4$  cm, for all subjects except 4. This is an indication that in transmittance mode a larger part of the fibrous, collagen-rich mammary gland is sampled, giving rise to higher overall scattering as well as a higher value of the slope factor  $b$ .

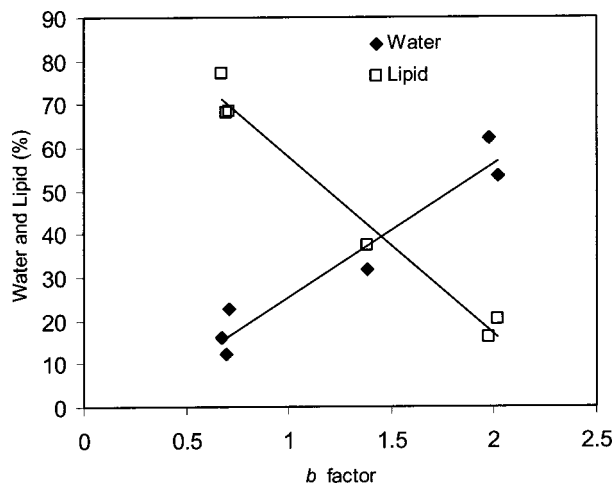
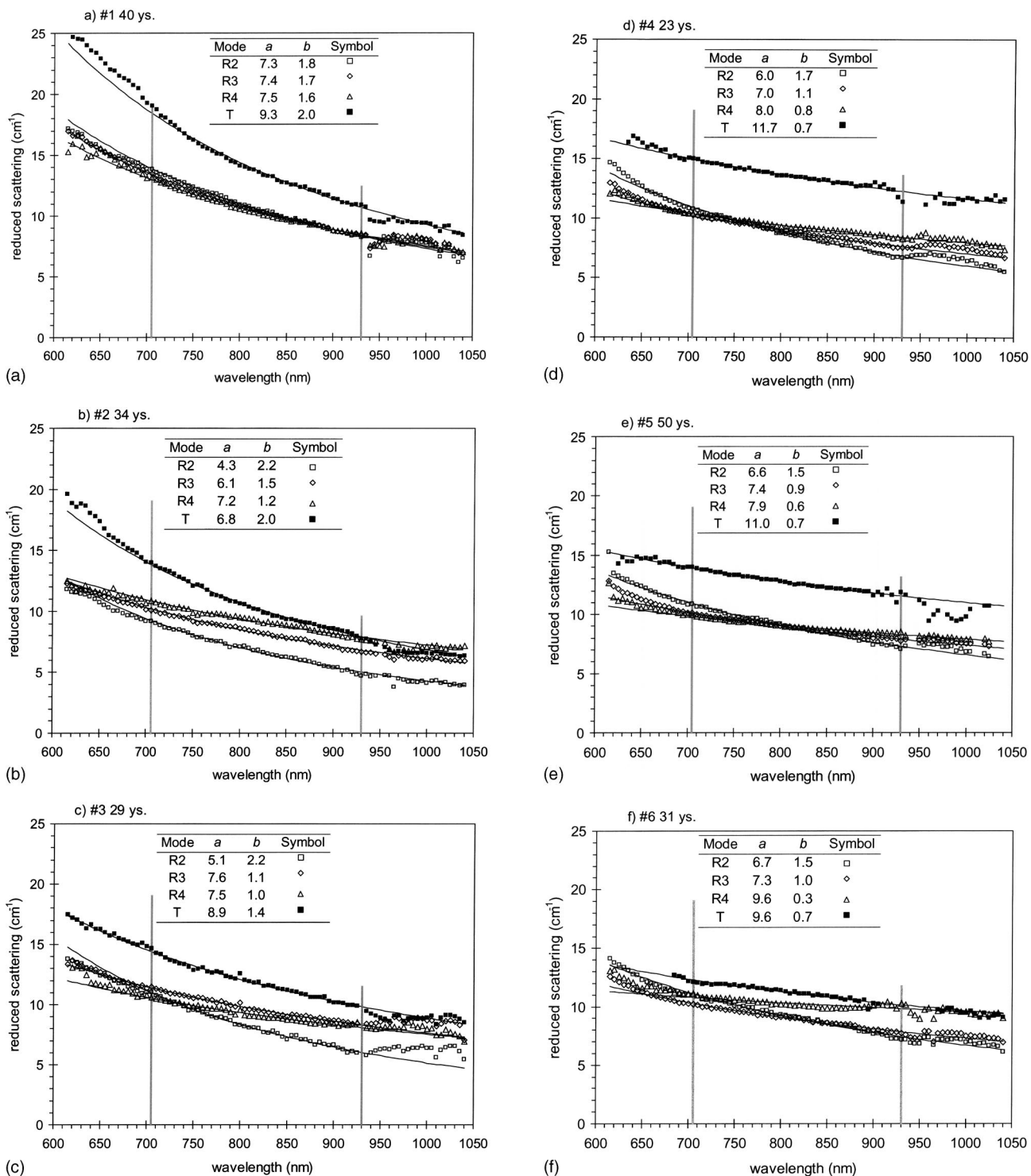


Fig. 6 Correlation plot of water and lipid content versus slope coefficient  $b$ .

We observe that there are larger differences between the measurement geometries in the scattering data than in the absorption data. This could be explained by the use of the homogenous tissue model and different spatial localization in the evaluation of  $\mu_a$  and  $\mu'_s$ . It is well known that the determination of  $\mu'_s$  is largely sensitive to the rising part of the time-dispersion curve, i.e., the early light, while most of the information about  $\mu_a$  is in the late part of the detected light.<sup>22,35</sup> This means that  $\mu_a$  has a larger effective sampling volume than  $\mu'_s$ , because the late light has had time to propagate over a larger volume. For the breast measurements, this interpretation means that the values of  $\mu_a$  comprise an average over a large part of the heterogeneous breast tissue, leading to similar values for all geometries. The evaluated values of  $\mu'_s$ , on the other hand, are more spatially localized and it is possible to see the influence of the dermis layer for short interfiber distances and the presence of the mammary gland for the transmittance measurement.

#### 4 Summary and Conclusions

In summary, we present the first, to our knowledge, investigation of *in-vivo* broad-spectrum measurements of breast tissue using different interfiber distances as well as transmittance measurements. These different measurement geometries imply that different volumes of the tissue are probed by the diffusely propagating light. Specifically, increasing the interfiber distance means deeper sampling depth, and the transmittance mode samples deeper core structures of the breast. The effects of the different sampling volumes and the nonhomogeneous tissue structures in the breast are not trivial to interpret. Nevertheless, we show that the measured parameters



**Fig. 7** All reduced scattering spectra: (a) subject 1, 40 years old; (b) subject 2, 34 years old; (c) subject 3, 29 years old; (d) subject 4, 23 years old; (e) subject 5, 50 years old; and (f) subject 6, 31 years old.

predominantly correlate with the breast type, water-rich or lipid-rich, but that small differences are also present that are a result of the different sampling volumes and the structures that are sampled within the breast in each specific case. The scattering spectra are more sensitive to the measurement mode—localization of the sampling volume—while the absorption spectra are less sensitive. As a next point, we see that

the influence on the absorption by water and lipid is significant even in the wavelength range 700 to 850 nm, which is the region primarily used for determining hemoglobin concentration and oxygen saturation. We have also pointed out the existence of a quasi-isosbestic point at 930 nm, where the absorption of breast tissue is largely independent of the relative amounts of lipid and water in the tissue. Furthermore, our

measurements indicate that when using hand-held probes, one has to be careful not to contaminate the signal with absorption from the chest muscle.

### Acknowledgments

The authors would like to thank Tomas Svensson for help with the laboratory work. The work was partially supported by the EU grants HPRI-CT-2001-00148, QLG1-CT-2000-00690, and QLG1-CT-2000-01464. Chikoidze acknowledges support by the TRIL program, Trieste, Italy.

### References

1. R. Berg, O. Jarlman, and S. Svanberg, "Medical transillumination imaging using short-pulse diode lasers," *Appl. Opt.* **32**, 574–579 (1993).
2. S. Fantini, S. A. Walker, M. A. Franceschini, M. Kaschke, P. M. Schlag, and K. T. Moesta, "Assessment of the size, position, and optical properties of breast tumors *in vivo* by noninvasive optical methods," *Appl. Opt.* **37**, 1982–1989 (1998).
3. D. Grosenick, K. T. Moesta, H. Wabnitz, J. Mucke, C. Stroszczyński, R. Macdonald, P. M. Schlag, and H. Rinneberg, "Time-domain optical mammography: initial clinical results on detection and characterization of breast tumors," *Appl. Opt.* **42**, 3170–3186 (2003).
4. B. J. Tromberg, N. Shah, R. Lanning, A. Cerussi, J. Espinoza, T. Pham, L. O. Svaasand, and J. Butler, "Non-invasive *in vivo* characterization of breast tumors using photon migration spectroscopy," *Neoplasia* **2**, 26–40 (2000).
5. J. C. Hebden, H. Veenstra, H. Dehghani, E. M. C. Hillman, M. Schweiger, S. R. Arridge, and D. T. Delpy, "Three-dimensional time-resolved optical tomography of a conical breast phantom," *Appl. Opt.* **40**, 3278–3287 (2001).
6. C. H. Schmitz, M. Locker, J. M. Lasker, A. H. Hielscher, and R. L. Barbour, "Instrumentation for fast functional optical tomography," *Rev. Sci. Instrum.* **73**, 429–439 (2002).
7. A. Pifferi, P. Taroni, A. Torricelli, F. Messina, R. Cubeddu, and G. Danesini, "Four-wavelength time-resolved optical mammography in the 680–980-nm range," *Opt. Lett.* **28**, 1138–1140 (2003).
8. B. W. Pogue, S. P. Poplack, T. O. McBride, W. A. Wells, K. S. Osterman, U. L. Osterberg, and K. D. Paulsen, "Quantitative hemoglobin tomography with diffuse near-infrared spectroscopy: pilot results in the breast," *Radiology* **218**, 261–266 (2001).
9. S. J. Matcher, C. E. Elwell, C. E. Cooper, M. Cope, and D. T. Delpy, "Performance comparison of several published tissue near-infrared spectroscopy algorithms," *Anal. Biochem.* **227**, 54–68 (1995).
10. T. O. McBride, B. W. Pogue, S. Poplack, S. Soho, W. A. Wells, S. Jiang, U. L. Osterberg, and K. D. Paulsen, "Multispectral near-infrared tomography: a case study in compensating for water and lipid content in hemoglobin imaging of the breast," *J. Biomed. Opt.* **7**, 72–79 (2002).
11. N. Shah, A. Cerussi, C. Eker, J. Espinoza, J. Butler, J. Fishkin, R. Hornung, and B. Tromberg, "Noninvasive functional optical spectroscopy of human breast tissue," *Proc. Natl. Acad. Sci. U.S.A.* **98**, 4420–4425 (2001).
12. E. L. Heffer and S. Fantini, "Quantitative oximetry of breast tumors: a near-infrared method that identifies two optimal wavelengths for each tumor," *Appl. Opt.* **41**, 3827–3839 (2002).
13. R. Cubeddu, A. Pifferi, P. Taroni, A. Torricelli, and G. Valentini, "Noninvasive absorption and scattering spectroscopy of bulk diffusive media: An application to the optical characterization of human breast," *Appl. Phys. Lett.* **74**, 874–876 (1999).
14. R. Cubeddu, C. D'Andrea, A. Pifferi, P. Taroni, A. Torricelli, and G. Valentini, "Effects of the menstrual cycle on the red and near infrared optical properties of the human breast," *Photochem. Photobiol.* **72**, 383–391 (2000).
15. A. E. Cerussi, A. J. Berger, F. Bevilacqua, N. Shah, D. Jakubowski, J. Butler, R. F. Holcombe, and B. J. Tromberg, "Sources of absorption and scattering contrast for near-infrared optical mammography," *Acta Radiol.* **8**, 211–218 (2001).
16. A. E. Cerussi, D. Jakubowski, N. Shah, F. Bevilacqua, R. Lanning, A. J. Berger, D. Hsiang, J. Butler, R. F. Holcombe, and B. J. Tromberg, "Spectroscopy enhances the information content of optical mammography," *J. Biomed. Opt.* **7**, 60–71 (2002).
17. S. Srinivasan, B. W. Pogue, S. Jiang, H. Dehghani, C. Kogel, S. Soho, J. J. Gibson, T. D. Tosteson, S. P. Poplack, and K. D. Paulsen, "Interpreting hemoglobin and water concentration, oxygen saturation, and scattering measured *in vivo* by near-infrared breast tomography," *Proc. Natl. Acad. Sci. U.S.A.* **100**, 12349–12354 (2003).
18. T. Durduran, R. Choe, J. P. Culver, L. Zubkov, M. J. Holboke, J. Giammarco, B. Chance, and A. G. Yodh, "Bulk optical properties of healthy female breast tissue," *Phys. Med. Biol.* **47**, 2847–2861 (2002).
19. S. J. Madsen, E. R. Anderson, R. C. Haskell, and B. J. Tromberg, "Portable, high-bandwidth frequency-domain photon migration instrument for tissue spectroscopy," *Opt. Lett.* **19**, 1934–1936 (1994).
20. M. A. Franceschini, K. T. Moesta, S. Fantini, G. Gaida, E. Gratton, H. Jess, W. W. Mantulin, M. Seeber, P. M. Schlag, and M. Kaschke, "Frequency-domain techniques enhance optical mammography: initial clinical results," *Proc. Natl. Acad. Sci. U.S.A.* **94**, 6468–6473 (1997).
21. S. Andersson-Engels, R. Berg, O. Jarlman, and S. Svanberg, "Time-resolved transillumination for medical diagnostics," *Opt. Lett.* **15**, 1179–1181 (1990).
22. R. Cubeddu, M. Musolino, A. Pifferi, P. Taroni, and G. Valentini, "Time resolved reflectance: a systematic study for the application to the optical characterization of tissue," *IEEE J. Quantum Electron.* **30**, 2421–2430 (1994).
23. M. S. Patterson, B. Chance, and B. C. Wilson, "Time resolved reflectance and transmittance for the non-invasive measurement of optical properties," *Appl. Opt.* **28**, 2331–2336 (1989).
24. R. Cubeddu, A. Pifferi, P. Taroni, A. Torricelli, and G. Valentini, "Experimental test of theoretical models for time-resolved reflectance," *Med. Phys.* **23**, 1625–1633 (1996).
25. J. Swartling, J. S. Dam, and S. Andersson-Engels, "Comparison of spatially and temporally resolved diffuse-reflectance measurement systems for determination of biomedical optical properties," *Appl. Opt.* **42**, 4612–4620 (2003).
26. R. C. Haskell, L. O. Svaasand, T. T. Tsay, T. C. Feng, M. S. McAdams, and B. J. Tromberg, "Boundary conditions for the diffusion equation in radiative transfer," *J. Opt. Soc. Am. A* **11**, 2727–2741 (1994).
27. K. Furutsu and Y. Yamada, "Diffusion approximation for a dissipative random medium and the applications," *Phys. Rev. E* **50**, 3634–3640 (1994).
28. W. H. Press, S. A. Teukolsky, W. T. Vetterling, and B. P. Flannery, *Numerical Recipes in C: The Art of Scientific Computing*, Cambridge University Press, New York (1992).
29. G. M. Hale and M. R. Querry, "Optical constants of water in the 200-nm to 200- $\mu$ m wavelength region," *Appl. Opt.* **12**, 555–563 (1973).
30. J. R. Mourant, T. Fuselier, J. Boyer, T. M. Johnson, and I. J. Bigio, "Predictions and measurements of scattering and absorption over broad wavelength ranges in tissue phantoms," *Appl. Opt.* **36**, 949–957 (1997).
31. A. M. K. Nilsson, C. Stureson, D. L. Liu, and S. Andersson-Engels, "Changes in spectral shape of tissue optical properties in conjunction with laser-induced thermotherapy," *Appl. Opt.* **37**, 1256–1267 (1998).
32. V. Quaresima, S. J. Matcher, and M. Ferrari, "Identification and quantification of intrinsic optical contrast for near-infrared mammography," *Photochem. Photobiol.* **67**, 4–14 (1998).
33. A. Torricelli, A. Pifferi, P. Taroni, E. Giambattistelli, and R. Cubeddu, "In vivo optical characterization of human tissues from 610 to 1010 nm by time-resolved reflectance," *Phys. Med. Biol.* **46**, 2227–2237 (2001).
34. S. Jiang, B. W. Pogue, K. D. Paulsen, C. Kogel, and S. P. Poplack, "In vivo near-infrared spectral detection of pressure-induced changes in breast tissue," *Opt. Lett.* **28**, 1212–1214 (2003).
35. S. Andersson-Engels, R. Berg, and S. Svanberg, "Effects of optical constants on time-gated transillumination of tissue and tissue-like media," *J. Photochem. Photobiol., B* **16**, 155–167 (1992).